Molecular Cell
Article

MSL Complex Is Attracted to Genes Marked by H3K36 Trimethylation Using a Sequence-Independent Mechanism

Erica Larschan,[1,2,3,6] Artyom A. Alekseyenko,[1,2,3,6] Andrey A. Gortchakov,[1,2,3] Shouyong Peng,[1,2,3,4] Bing Li,[5] Pok Yang,[1,2,3] Jerry L. Workman,[5] Peter J. Park,[2,4] and Mitzi I. Kuroda[1,2,3,*]
[1]Howard Hughes Medical Institute
[2]Harvard Partners Center for Genetics and Genomics
Brigham and Women's Hospital, 75 Francis Street, Boston, MA 02115, USA
[3]Department of Genetics, Harvard Medical School, 77 Avenue Louis Pasteur, Boston, MA 02115, USA
[4]Children's Hospital Informatics Program, Children's Hospital, 320 Longwood Avenue, Boston, MA 02115, USA
[5]Stowers Institute for Medical Research, 1000 East 50th Street, Kansas City, MO 64110, USA
[6]These authors contributed equally to this work.
*Correspondence: mkuroda@genetics.med.harvard.edu
DOI 10.1016/j.molcel.2007.08.011

SUMMARY

In *Drosophila*, X chromosome dosage compensation requires the *m*ale-specific *l*ethal (MSL) complex, which associates with actively transcribed genes on the single male X chromosome to upregulate transcription ~2-fold. We found that on the male X chromosome, or when MSL complex is ectopically localized to an autosome, histone H3K36 trimethylation (H3K36me3) is a strong predictor of MSL binding. We isolated mutants lacking *Set2*, the H3K36me3 methyltransferase, and found that *Set2* is an essential gene in both sexes of *Drosophila*. In *set2* mutant males, MSL complex maintains X specificity but exhibits reduced binding to target genes. Furthermore, recombinant MSL3 protein preferentially binds nucleosomes marked by H3K36me3 in vitro. Our results support a model in which MSL complex uses high-affinity sites to initially recognize the X chromosome and then associates with many of its targets through sequence-independent features of transcribed genes.

INTRODUCTION

Dosage compensation is an essential process that functions to equalize the levels of transcripts encoded on the X chromosome in heterogametic organisms. In mammals, dosage compensation occurs by inactivation of one of the two female X chromosomes (Ng et al., 2007; Yang and Kuroda, 2007). In *Drosophila*, dosage compensation requires the *m*ale-specific *l*ethal (MSL) complex, which upregulates transcription on the single male X chromosome (Straub and Becker, 2007). MSL targeting provides a model for understanding how chromatin modification complexes identify and target active genes. At least five proteins, collectively called MSL proteins, and two *roX* (RNA on X) noncoding RNAs are components of MSL complex. MSL proteins are thought to assemble on nascent *roX* transcripts, encoded by the *roX1* and *roX2* genes on the X chromosome. In addition, ~35–60 high-affinity sequences are proposed to contribute to the specific identity of the X chromosome, presumably through DNA recognition motifs (Kelley et al., 1999; Demakova et al., 2003). Initial targeting of MSL complex to the X might be followed by binding to additional, lower-affinity DNA binding sites (Demakova et al., 2003; Fagegaltier and Baker, 2004; Legube et al., 2006; Dahlsveen et al., 2006) or by locating active genes on the same chromosome (Kelley et al., 1999; Alekseyenko et al., 2006).

Global mapping of MSL proteins on the X chromosome has demonstrated that MSL complex associates primarily with genes rather than intergenic regions and displays a 3′ bias (Alekseyenko et al., 2006; Gilfillan et al., 2006). In general, the MSL binding pattern is very similar in distinct cell types, correlating with stably transcribed genes (Alekseyenko et al., 2006). Rare examples of genes that are bound in one cell type but not another indicate that MSL complex preferentially associates with genes when they are transcribed (Alekseyenko et al., 2006). These data reinforce the correlation between transcription and binding, providing evidence that sequence elements alone are not sufficient for MSL complex recruitment. Therefore, we hypothesized that general factors associated with transcription units and skewed toward 3′ ends of transcribed genes may be involved in MSL complex binding and/or stabilization.

Covalent modification of histone tails is a highly conserved mechanism by which organisms distinguish active and repressed regions of the genome. Many histone modifications are known to be associated with transcribed genes to modulate transcription and differentiate transcribed genes from silenced ones (Jenuwein and Allis, 2001; Bernstein et al., 2007; Rando, 2007). The MSL3 component of MSL complex contains a chromodomain, and in several cases chromodomain proteins interact directly with methylated histone tails (Daniel et al., 2005).

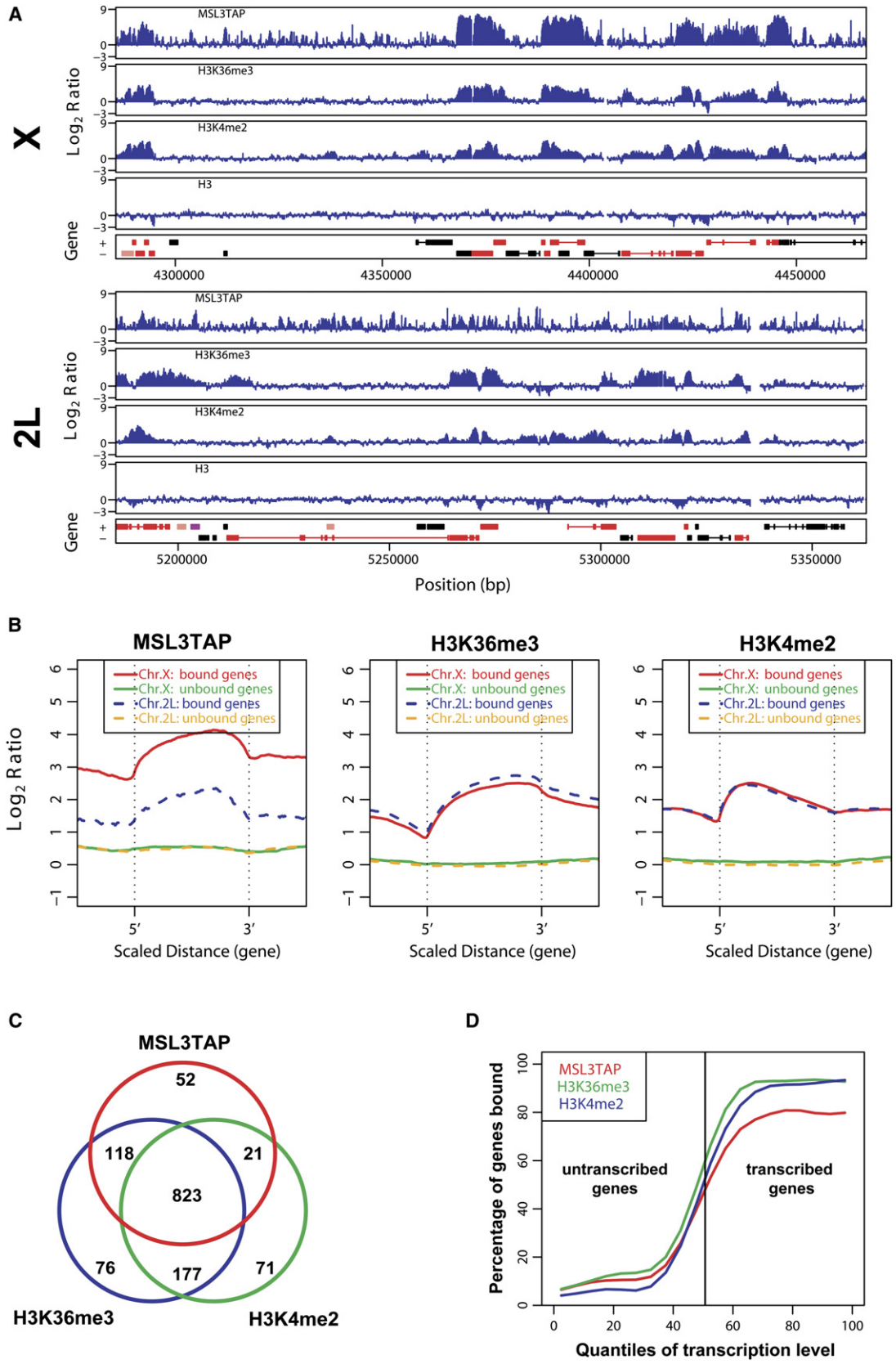
A
X
2L
MSL3TAP
H3K36me3
H3K4me2
H3
Log2 Ratio
Gene
4300000
4350000
4400000
4450000
5200000
5250000
5300000
5350000
Position (bp)
B
MSL3TAP
H3K36me3
H3K4me2
Chr.X: bound genes
Chr.X: unbound genes
Chr.2L: bound genes
Chr.2L: unbound genes
Log2 Ratio
5′
3′
Scaled Distance (gene)
C
MSL3TAP
52
118
21
823
76
177
71
H3K36me3
H3K4me2
D
MSL3TAP
H3K36me3
H3K4me2
untranscribed genes
transcribed genes
Percentage of genes bound
Quantiles of transcription level

The H3K36me3 modification is the only known methylation mark in yeast or human that exhibits a 3′ bias in binding to transcribed genes, suggesting a potential to attract MSL complex in *Drosophila* (Liu et al., 2005; Barski et al., 2007). Furthermore, several recent reports identified a physical and functional interaction between the H3K36me3 and the *S. cerevisiae* Eaf3 protein, an MSL3 homolog that is a component of the Rpd3(S) histone deacetylase complex (Carrozza et al., 2005; Joshi and Struhl, 2005; Keogh et al., 2005). Rpd3(S) deacetylates histones in the wake of RNA polymerase II to prevent inaccurate initiation. In *S. cerevisiae*, H3K36me3 is catalyzed by the Set2 protein, which has roles in transcriptional repression via inhibiting TBP recruitment and suppression of aberrant transcriptional start sites (Strahl et al., 2002; Biswas et al., 2006; Carrozza et al., 2005). In *S. cerevisiae*, *S. pombe*, *Neurospora crassa*, and NIH 3T3 cells, weak slow-growth phenotypes have been observed when H3K36me3 is lost, indicating a requirement for H3K36me3 during cell growth (Strahl et al., 2002; Adhvaryu et al., 2005; Brown et al., 2006).

The function of H3K36me3 in *Drosophila* had not been analyzed. In this study, we identify a function for H3K36me3 in MSL complex recruitment to active genes on the X chromosome in addition to an essential role in both sexes. We find that when MSL complex is ectopically localized to an autosome, its binding displays the same characteristics as MSL targets on X: it is bound to transcribed genes with a 3′ bias, correlating with H3K36me3. Furthermore, we demonstrate that MSL3 preferentially binds to nucleosomes marked by H3K36me3 in vitro. Our results support a model in which MSL complex recognizes many of its targets through general features of transcribed genes rather than relying on specific, enriched *cis*-acting sequences.

RESULTS

MSL Complex Colocalizes with H3K36 Trimethylation on X-Linked Genes

To investigate the relationship between MSL complex recruitment and histone methylation, ChIP-on-chip analysis of SL2 cells was performed with antibodies that recognize H3 trimethylated at K36 (H3K36me3) or dimethylated at K4 (H3K4me2) (Figure 1A). The SL2 cell line exhibits a male phenotype with respect to dosage compensation (Hamada et al., 2005). We used NimbleGen tiling arrays that contained the entire X chromosome and left arm of chromosome 2, tiled at 100 bp resolution (Alekseyenko et al., 2006). A general histone H3 antibody was used as a control for histone occupancy, and three biological replicates for tiling arrays indicated a high degree of reproducibility (see Figure S1 in the Supplemental Data available with this article online). As expected, the H3K36me3 and H3K4me2 modifications were associated with the 3′ and 5′ ends of transcribed genes, respectively, as previously reported for *S. cerevisiae*, mammals, and chicken (Bannister et al., 2005; Pokholok et al., 2005; Vakoc et al., 2006) (Figures 1B and 1D, Figures S2 and S3). We found that close to 100% of transcribed genes on the X and 2L chromosomes were methylated at H3K36 and H3K4, largely independent of transcript level as previously reported for other organisms (Rao et al., 2005; Kim et al., 2007) (Figures 1A and 1D, Figure S3). Similar results were observed for MSL3-TAP, specifically on the X chromosome, but a lower fraction of transcribed genes on the X was bound (approximately 80%) (Figure 1D). With improved computational analysis, we currently score 1014 genes on the X chromosome positive for MSL binding in SL2 cells (up from our previous estimate of 675 genes). Our new computational approach obviates the need to make assumptions about the appropriate threshold or use a mock control, and it accurately corrects for dye bias (Peng et al., 2007). Furthermore, 67% of the newly scored MSL-bound genes in SL2 cells were identified previously as clearly bound in at least one cell type (Alekseyenko et al., 2006).

To determine whether MSL binding colocalizes with H3K36me3 or H3K4me2, we examined the correlation between the data sets at the gene level. Of the 1014 MSL-bound genes in SL2 cells, 93% were positive for H3K36me3, and 83% were positive for H3K4me2 (Figure 1C). Interestingly, we previously reported that a small percentage of untranscribed genes were bound by MSL3-TAP (7%), and here we found that these genes also carried the H3K36me3 histone modification (Figure S3).

Figure 1. MSL Complex Colocalizes with H3K36me3 on the Middle and 3′ Ends of Transcribed Genes in SL2 Cells

(A) H3K36me3, H3K4me2, and MSL complex localize to transcribed genes by ChIP-on-chip analysis in SL2 cells. ChIP-on-chip profiles shown are generated from NimbleGen tiling arrays. Genes are color coded based on their transcription status (red, transcribed; black, nontranscribed; pink and magenta, genes that are differentially transcribed between S2 and clone 8 cells). Top row genes are transcribed left to right, and bottom row genes are transcribed from right to left. Numbers along the x axis refer to chromosomal position, and the units are base pairs along the X or 2L chromosomes. The y axis shows the log ratio of IP/IN ChIP-on-chip signal and is shown with a log scale. Binding sites are defined as clusters of more than eight consecutive probes. Therefore, no MSL binding sites are observed on the 2L region shown.

(B) H3K36me3 and MSL complex have a 3′ bias to their average gene profiles. In contrast, H3K4me2 has a 5′ bias. An average gene profile was compiled after identification of bound genes using statistical approaches (Experimental Procedures). In SL2 cells only (not in embryos or larvae), a small number of contiguous genes on 2L are bound by MSL complex, possibly due to a translocation (Alekseyenko et al., 2006).

(C) Genes that exhibit H3K36me3, H3K4me2, and MSL complex binding show a high degree of correlation, as shown by a Venn diagram.

(D) H3K36me3, H3K4me2, and MSL complex binding to transcribed genes largely independent of transcription level. All genes on the X chromosome were binned into ten quantiles based on transcript level determined from Affymetrix microarrays (x axis) (Alekseyenko et al., 2006). Using Affymetrix present or absent designations, genes that were called absent are referred to as nontranscribed (left of vertical black line), and genes that were called present are referred to as transcribed (right of vertical black line). The y axis shows the average binding frequency for all genes in each quantile for each protein or histone modification: (1) MSL3-TAP (red line), (2) H3K36me3 (green line), and (3) H3K4me2 (blue line).

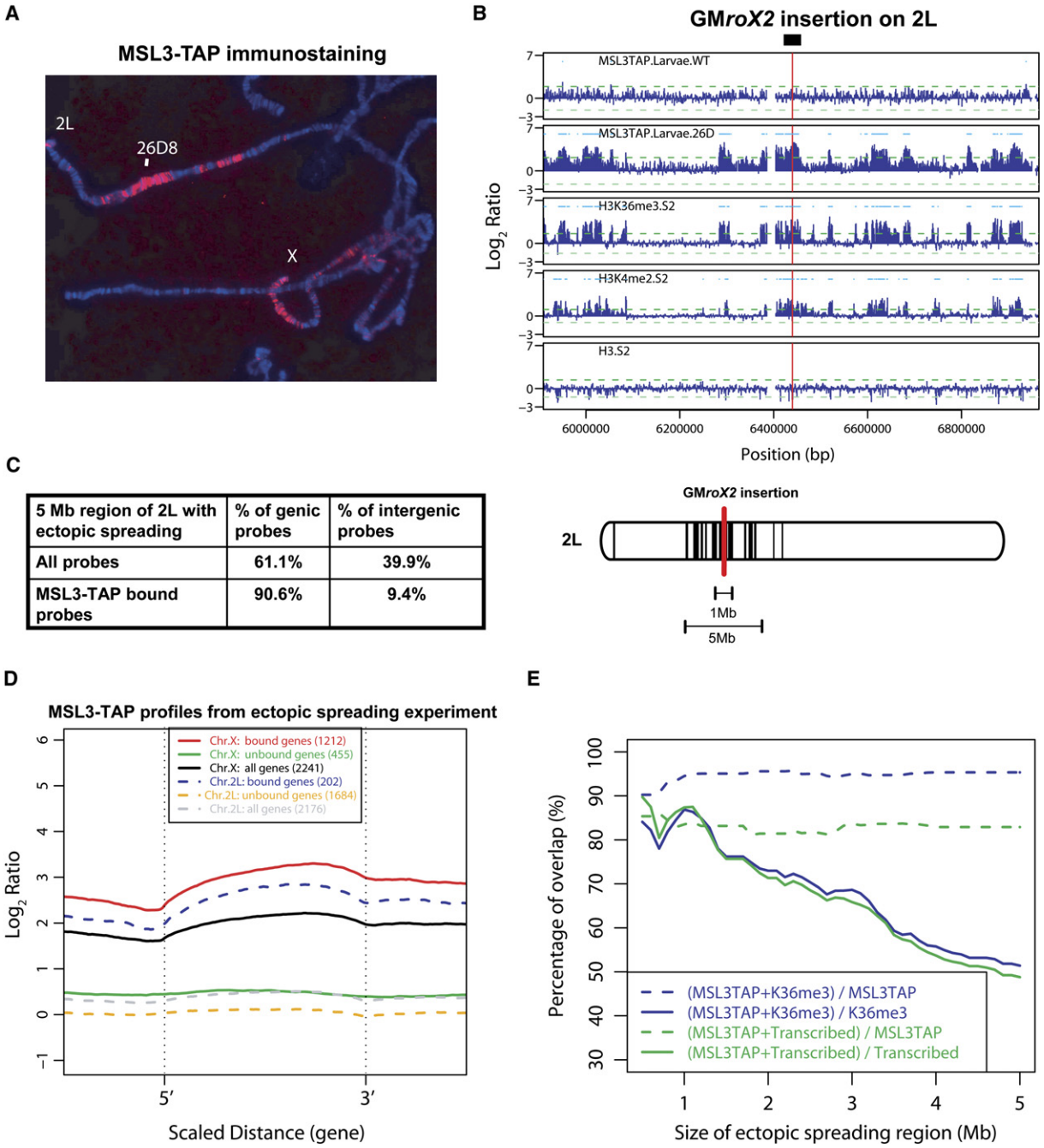

5 Mb region of 2L with ectopic spreading	% of genic probes	% of intergenic probes
All probes	61.1%	39.9%
MSL3-TAP bound probes	90.6%	9.4%

Figure 2. Ectopic Binding of MSL Complex Surrounding an Insertion of the *roX2* Gene on Chromosome 2L

(A) Immunostaining for MSL3-TAP (red) on polytene chromosomes from male larvae containing the *roX2* gene inserted at cytological position 26D8 on chromosome 2L. DAPI staining of the DNA is shown in blue. "X" marks the tip of the X chromosome, and "2L" marks the tip of the 2L chromosome arm. The full genotype was *y w roX1*^{ex6} *Df (1)roX2*^{52} *P[w+4Δ4.3]; P[w+ GMroX2-pFRT]/P[w+ MSL3-TAP-pCaSpeR3-1]; msl3*^{1} /+.

(B) ChIP-on-chip profiles for MSL3-TAP from wild-type males that do not contain a *roX2* insertion on 2L (top row) and males with *roX2* inserted at 26D (second row) (top panel). The *roX2* insertion site is depicted as a red line. Profiles are also shown for H3K36me3, H3K4me2, and H3 from SL2 cells. The x axis is position in bp along the 2L chromosome, and the y axis is the log ratio of IP/IN signal and is shown with a log scale as in Figure 1 (top panel). The horizontal dotted blue lines indicate the thresholds above which a bound cluster is scored positive. The bottom panel shows a scaled schematic of chromosome 2L with MSL3-TAP binding sites shown as vertical black lines.

(C) Within a 5 Mb region surrounding the *roX2* insertion site, MSL3-TAP-bound probes are strongly enriched for genic regions when compared with intergenic regions (bottom row). The distribution of all probes (oligos on the array) is indicated above.

In addition, untranscribed genes bound by MSL have significantly higher levels of H3K36me3 than untranscribed genes that are unbound by MSL complex (Figure S4). A likely explanation is that some nontranscribed genes are located near transcribed genes with very extensive H3K36me3 and MSL signals or within domains that have continuous strong signal over many kilobases. Specifically, 82% of MSL3-TAP-bound genes are transcribed, while 93% percent of MSL3-TAP-bound genes carry the H3K36me3 modification (Figure S3). Therefore, H3K36me3 is an even better predictor of MSL binding on the X than transcription state as defined by Affymetrix expression arrays. Similar results were observed for clone 8 cells, a *Drosophila* cell line derived from the wing disc (data not shown).

Colocalization in terms of whole genes could occur without coincident binding along the gene. We previously reported that MSL3-TAP binds over the body of transcribed genes specifically on the X chromosome with a bias toward the 3′ end (Alekseyenko et al., 2006) (Figure 1B, Figure S2). To determine whether H3K36me3 on the X chromosome and MSL complex colocalize spatially within transcription units, we compared average gene profiles for H3 methylation modifications and MSL3-TAP. We found that H3K36me3 and MSL3-TAP exhibit a similar 3′ biased profile, whereas H3 lysine 4 dimethylation is associated with the 5′ end of transcription units, as reported in other organisms (Figure 1B, Figure S2). Furthermore, at the probe level, a strong positive correlation is observed between MSL binding and H3K36me3 association (Figure S4). In contrast, a weaker correlation is observed with H3K4me2 that associates with the 5′ ends of genes (Figure 1B, Figure S4). Our results demonstrate that H3K36 trimethylation is a 3′ biased mark associated generally with active transcription units and that it is a very strong predictor of MSL binding on the X chromosome.

MSL Complex Attracted to Chromosome 2L by a *roX2* Transgene Binds Neighboring 2L Genes Marked by Transcription and H3K36me3

When either a *roX1* or a *roX2* genomic transgene is inserted on an autosome, it attracts MSL complex to its site of insertion, with occasional signs of additional binding to neighboring regions along the autosome. Ectopic binding along the autosome is greatly increased when the X chromosome in the same nucleus is deleted for both *roX1* and *roX2* (Park et al., 2002). Such binding generally extends >1 Mb bidirectionally from the site of the *roX* transgene insertion, as measured by immunofluorescence for the MSL proteins. One interpretation is that nascent *roX* RNAs compete for attraction of the MSL proteins for assembly at their site of synthesis and that, after local assembly, MSL complex becomes competent to search for targets in its new chromosome environment. To determine whether ectopic binding on a normally untargeted chromosome would provide clues to the specificity of MSL binding, we performed ChIP-on-chip analysis on MSL3-TAP male larvae mutant for both *roX1* and *roX2* on the X chromosome and containing a *roX2* transgene inserted at position 26D8-9 (near the *CG9537* gene) on chromosome 2L. When assayed by immunostaining of polytene chromosomes, such males consistently show MSL binding in interbands along chromosome 2L, surrounding the site of the transgene insertion (Figure 2A). At the level of genomic tiling arrays, our ChIP results map this binding at high resolution. As a control, we used an additional array that contains the 3R chromosome and the entire X (see the Experimental Procedures). We found that the domain of MSL binding extends greater than 2 Mb in each direction from the insertion site on 2L (Figure 2B), while binding to 3R was undetected (data not shown). Importantly, the targets of binding are transcribed 2L genes, with the averaged binding profile showing enrichment over the bodies of genes, with a bias toward 3′ ends (Figures 2B–2D). Each of these characteristics is typical of target genes on the X chromosome in wild-type larvae, cells, and embryos. Furthermore, when we compared the 2L pattern of ectopic MSL binding in larvae to the wild-type distribution of H3K36 trimethylation in tissue culture cells, we found a strong correlation between MSL binding and K36me3 within 1 Mb of the site of the *roX* transgenic insertion (Figure 2E). Interestingly, although MSL-bound genes are consistently marked with H3K36me3, at greater than 1 Mb distances from the transgene insertion site, MSL complex increasingly skips some H3K36me3-bound genes while binding others (Figure 2E). Overall, we found that MSL targets selected on 2L were transcribed genes enriched for H3K36 trimethylation and that MSL binding showed a 3′ bias analogous to that normally found on X chromosome targets (Figures 2B–2D). These results raise the strong possibility that, once targeted to a chromosomal domain by a high-affinity site, MSL complex recognizes general marks for transcription such as H3K36me3 or other 3′-associated features rather than an X-specific sequence element at each individual target.

(D) Average gene profiles for MSL3-TAP binding to 2L indicate a 3′ bias similar to that noted on the wild-type X chromosome. Profiles of clearly bound and clearly unbound genes are shown as defined in the Experimental Procedures.

(E) MSL3-TAP binding sites on 2L correlate with sites of H3K36me3 modification and transcribed genes. The y axis shows the following: (1) percent of MSL3-TAP binding sites that are also bound by H3K36me3 (dashed blue line); (2) percent of MSL3-TAP binding sites that are also transcribed genes (dashed green line); (3) percent of H3K36me3-modified regions that are also bound by MSL3-TAP (solid blue line); and (4) percent of transcribed genes that are also bound by MSL3-TAP (solid green line). The x axis represents the size of the region of ectopic spreading on 2L used to calculate the percentage overlap plotted on the y axis. As the size window for ectopic spreading increases (x axis), fewer H3K36me3-modified regions and transcribed genes are bound by MSL3-TAP, but most MSL3-TAP-bound probes are still located in regions that are modified at H3K36me3 and transcribed. Also, there is a better correlation between MSL3-TAP binding and H3K36me3 modification (dashed blue line), similar to what was observed for the X chromosome (Figure 1C).

Set2 Is Required for H3K36 Trimethylation and for Viability in Both Males and Females in *Drosophila melanogaster*

To investigate whether H3K36me3 plays a functional role in MSL complex targeting, we took a genetic approach to inactivate the methyltransferase responsible for H3K36me3 in *Drosophila*. In *S. cerevisiae*, the Set2 histone methyltransferase is responsible for di- and trimethylation of H3K36 (Rao et al., 2005; Strahl et al., 2002). Strahl and colleagues identified the *CG1716*-encoded protein as the likely functional homolog of ySet2 in *Drosophila* based on the presence of SRI and SET domains (Morris et al., 2005). We pursued two initial tests to examine *CG1716* function, the first in yeast and the second in *Drosophila* tissue culture cells. To test the function of *CG1716* in yeast, we transformed an inducible *CG1716* expression vector into *set2Δ* mutant *S. cerevisiae* that lack detectable H3K36me3 (Figure 3A). We found that when we induced *CG1716* by growth in media containing galactose, H3K36me3 (and some H3K36me2) was restored, demonstrating that a *CG1716* cDNA functionally complements the yeast *set2Δ*. Also, the *CG1716*-encoded protein can interact with the RNA Pol II CTD as observed for *S. cerevisiae* Set2, further confirming the identity of *CG1716* as the functional homolog of the *S. cerevisiae SET2* gene (Figure S5) (Vojnic et al., 2006). To test the function of *CG1716* in *Drosophila* tissue culture cells, we used RNAi to target *CG1716*. We found that a strong reduction of *CG1716* mRNA correlated with a significant loss of H3K36me3 by western blot, immunostaining, and ChIP analysis. H3K4me2, a distinct chromatin mark for transcribed genes, was largely unaffected (Figures 3B–3D). ChIP analysis allowed quantification of a 3- to 5-fold reduction in H3K36me3 and only very small changes in H3K4me2 (Figure 3E). Based on these results, we proceeded to isolate a *Drosophila* mutant that disrupts the *CG1716* gene, henceforth referred to as the *Set2* gene.

We induced imprecise excision of a P element upstream of the *Set2* gene to create a series of *Set2* deletion strains, and we selected $Set2^1$ for further analysis. $dSet2^1$ eliminates most of the coding region including the catalytic SET domain without extending bidirectionally into the neighboring *CG1998* gene (Figure 4A). Since the *Set2* gene is located on the X chromosome, we initially isolated hemizygous males and found that they died as late third-instar larvae. To demonstrate that this lethality was due to loss of *Set2*, and not to any additional defects that might have been induced during P element excision, we constructed a transgene encompassing only the genomic region of *Set2* and found that it was able to fully rescue the $Set2^1$ mutants (data not shown). Using the rescued males as fathers, we subsequently examined homozygous mutant females and found that the $Set2^1$ mutation causes late larval lethality in both sexes. To further analyze the viability of *Set2* mutants at the cellular level, we created homozygous mutant *Set2* eyes in the context of heterozygous mutant adult females, using the GMR-hid system (Stowers and Schwarz, 1999). *set2* mutant eyes were diminished in size and rough compared to wild-type eyes, which is a qualitative assay suggesting that *Set2* is important for normal cell proliferation (Figure 4B).

To determine whether or not H3K36me3 was affected in the *set2* mutant, we immunostained polytene chromosome squashes of mutant larvae (Figure 4C). We found that H3K36me3 was significantly depleted in the $Set2^1$ mutant when compared to wild-type. As a control for the specificity of this defect, we immunostained the same nuclei for the interband protein Z4, which showed similar staining in wild-type and mutant. We further analyzed $Set2^1$ mutant larvae by ChIP to quantify the H3K36me3 levels in wild-type and $Set2^1$ mutants. We found that H3K36me3 in the $Set2^1$ mutant was dramatically decreased at the transcribed genes tested, to levels comparable to an untranscribed gene (*CG15570*) (Figure 4D). Changes in H3K4me2 varied from slight to none. Thus, *Set2* is required for viability and methylation of H3K36 in *Drosophila*.

Set2 Contributes to Optimal MSL Complex Targeting at Transcribed Genes, but Not at High-Affinity Sites

To examine whether MSL complex targeting requires H3K36me3, we immunostained polytene chromosomes of $Set2^1$ mutant larvae with antibodies directed against MSL complex, but no difference in MSL pattern or intensity was detected at this level of resolution (data not shown). Upon initial consideration, this result would appear to rule out a requirement for H3K36me3 in MSL targeting. However, when we proceeded to validate this observation with ChIP assays conducted with two independent fly stocks and ChIP protocols (both anti-MSL2 and MSL3-TAP IPs), we found that wild-type and $Set2^1$ mutant larvae showed significant differences at many specific gene targets (Figures 5A and 5B). Nine genes with high, medium, or low levels of MSL complex binding were assayed for recruitment of MSL2 and MSL3-TAP in wild-type and $Set2^1$ mutant third-instar larvae by ChIP analysis. We observed highly reproducible 2- to 10-fold decreases in MSL2 and MSL3-TAP association at all nine genes assayed (Figures 5A and 5B). In contrast, MSL complex association with previously reported "high-affinity sites," such as *roX1*, *roX2*, and 18D11, was largely unaffected in the $Set2^1$ mutant (Figures 5A and 5B, left panels).

Such a result might be attributed to indirect effects in $Set2^1$ mutant larvae as opposed to specific defects in MSL targeting. To address this, we measured *roX* RNA and *msl2* mRNA levels and found that they were not affected significantly in the $Set2^1$ mutant, suggesting that H3K36me3 does not affect MSL complex recruitment indirectly by affecting expression of MSL components (Figure 5C). Western and polytene staining analysis of Msl1 and Msl2 also indicate that protein levels are largely unchanged (data not shown). We also found that ChIP for H3K4me2 (Figure 4D) and RNA polymerase II (Figure S6) were not significantly affected in *set2* mutants, further supporting a direct role for H3K36me3 in stabilization of MSL complex at target genes.

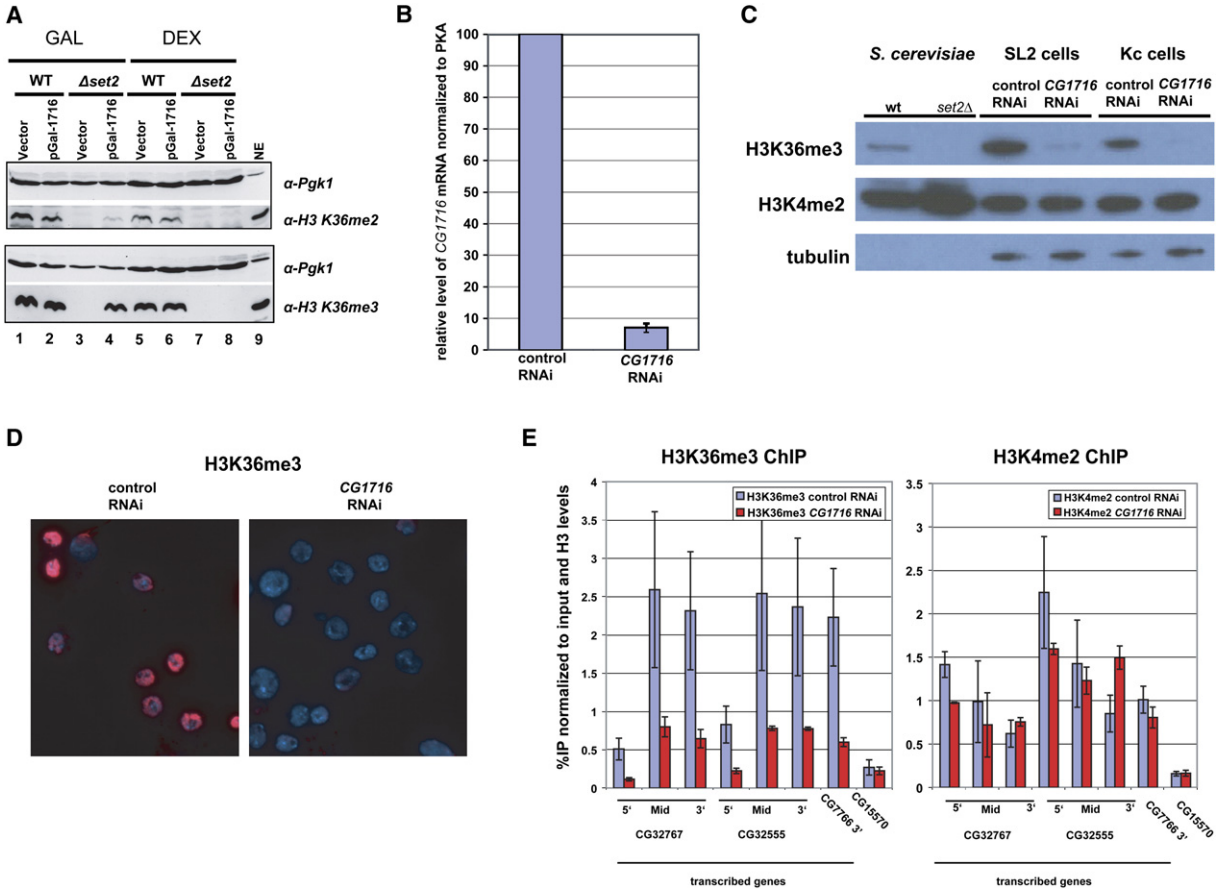

Figure 3. CG1716 Protein Can Functionally Complement the *S. cerevisiae set2Δ* and Is Important for H3K36me3 in *Drosophila* Tissue Culture Cells

(A) Expression of a *CG1716* cDNA can functionally complement the *S. cerevisiae set2Δ* for H3K36me3 levels (bottom panels) and partially complements the loss of H3K36me2 (top panels). The anti-Pgk-1 antibody is used as a loading control. GAL indicates inducing conditions for the *CG1716* cDNA and DEX indicates repressing conditions for the *CG1716* cDNA.

(B) *CG1716* RNAi reduces levels of *CG1716* mRNA as assayed by quantitative RT-PCR. Error bars shown are standard deviation.

(C) *CG1716* RNAi reduces H3K36me3 levels, but not H3K4me2 levels, as assayed by western blotting on S2 and Kc *Drosophila* cells.

(D) *CG1716* RNAi reduces H3K36me3 levels in S2 cells as assayed by immunostaining. H3K36me3 is localized to the nucleus in S2 cells.

(E) *CG1716* RNAi reduces H3K36me3 levels, but not H3K4me2, as assayed by ChIP, and both modifications are specific for transcribed genes. *CG15570* is an untranscribed gene. The error bars are defined as standard deviations of at least three experiments.

To address the functional role of H3K36me3 in transcription of genes bound by MSL complex, we compared the transcript levels of MSL complex target genes in wild-type and *Set2*^{1} mutant larvae. Transcription of MSL target genes is not strongly affected in *Set2*^{1} mutant larvae, although genes that exhibit the strongest loss of MSL complex binding (*CG13316*, *CG12690*, *CG32555*, and *CG32575*) exhibit decreases in transcript level (Figure S6). Dosage compensation involves a 2-fold upregulation of transcription, limiting the expected transcriptional changes to a 50% decrease in transcript. Furthermore, when we examined H4K16 acetylation at these genes, we found significant residual levels (10-fold over autosomal controls or untranscribed genes), even when very small amounts of MSL complex remain (Figure S6). Thus, residual MSL complex function may be largely sufficient for transcriptional upregulation in the *Set2*^{1} mutant, yet MSL complex targeting is significantly reduced.

Together, our results suggest that a subset of MSL binding sites is particularly sensitive to H3K36me3 levels, while others, including three previously defined high-affinity sites are not. Since MSL binding is diminished significantly but not ablated in the *Set2*^{1} mutant, our results support a model in which recognition of H3K36me3 is one contributing factor to MSL complex targeting that functions with additional features of transcribed genes.

An important caveat to the conclusion that H3K36me3 functions together with other recognition features is that the heterozygous mothers of hemizygous *Set2*^{1} mutants carry a functional *Set2* gene and thus could provide a

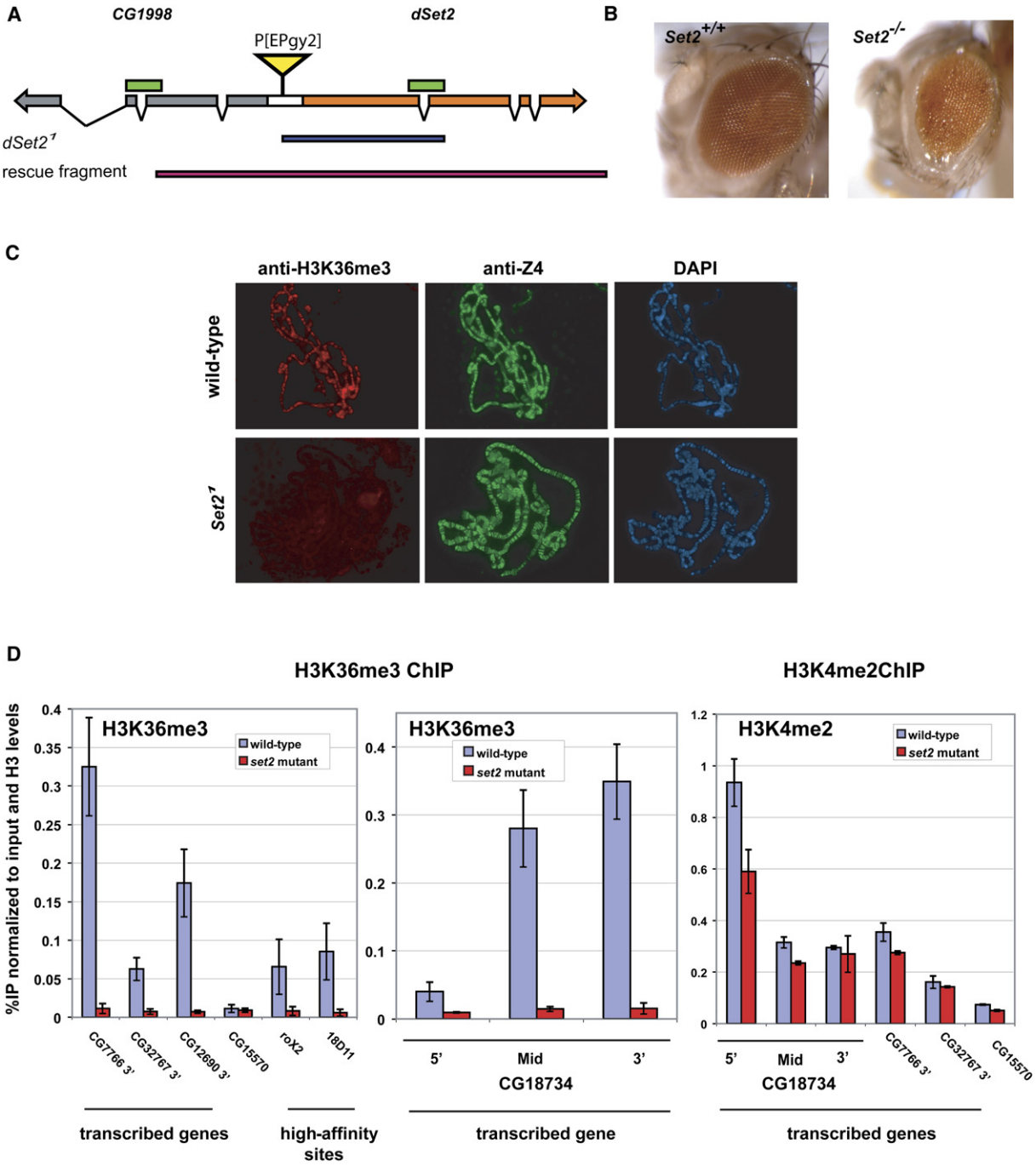

Figure 4. *Set2* Is Required for H3K36me3 In Vivo and Is Essential for Development Past the Larval Stage in Both Sexes

(A) Schematic of the *Set2* locus, P element insertion (yellow), deletion mutant (blue) obtained by imprecise excision, and rescue fragment (magenta). The green boxes represent highly conserved regions.

(B) The *Set2*^{1} mutant exhibits a cell-autonomous growth defect as observed by using the *GMR-hid* system to generate homozygous mutant fly eyes.

(C) The *Set2*^{1} mutant exhibits a significant loss of H3K36me3 on polytene chromosomes from third-instar larvae compared to the Z4 interband specific protein assayed as a control.

(D) The *Set2*^{1} mutant exhibits a significant loss of H3K36me3 as determined by ChIP in third-instar larvae. H3K4me2 is less affected by the *Set2*^{1} mutant. The error bars are defined as standard deviations of at least three experiments.

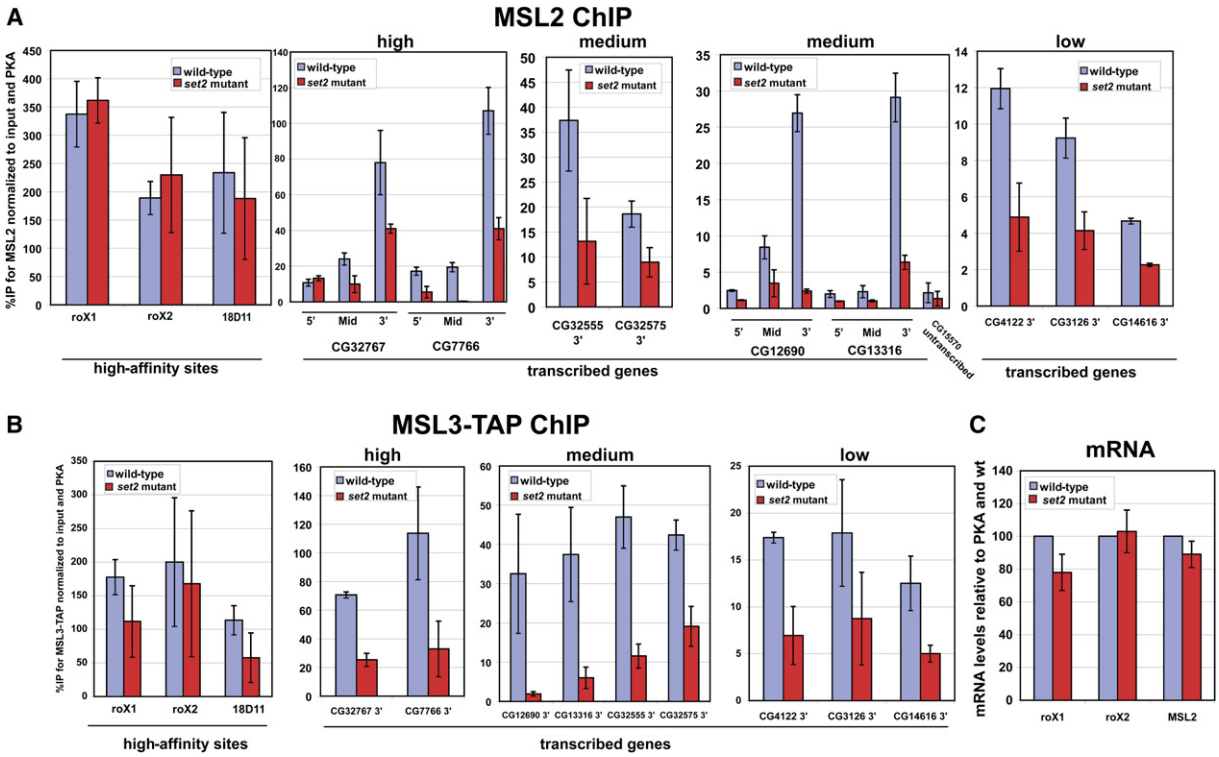

Figure 5. H3K36me3 Has a Role in Specifying MSL Complex Target Genes, but Not High-Affinity Sites

(A) MSL2 association with nine target genes is significantly reduced in the *Set2*^{1} mutant male larvae as assayed by ChIP. In contrast, MSL2 association with high-affinity sites remains largely unchanged. Target genes were identified from ChIP-on-chip analysis. All error bars shown are standard deviation.

(B) MSL3-TAP association with nine target genes is significantly reduced in the *Set2*^{1} mutant as assayed by ChIP. In contrast, MSL3-TAP association with high-affinity sites remains largely unaltered.

(C) mRNA levels of *roX1*, *roX2*, and *MSL2* are largely unchanged in *Set2*^{1} mutant male larvae.

The error bars are defined as standard deviations of at least three experiments.

maternal supply of wild-type *Set2* mRNA or protein to the mutant embryos. This maternal contribution of H3K36me3 could be sufficient to initially establish MSL binding, which might be maintained through development, independent of the initial recognition mark. Thus, if the maternal contribution of H3K36me3 could be eliminated, we hypothesized that we might observe an even more significant defect in MSL complex recruitment. To address this possibility genetically, we constructed a stock designed to create homozygous *set2* mutant germline clones using FLP-FRT-mediated recombination in an *ovo*^{D} dominant female sterile mutant (Chou and Perrimon, 1992). After recombination, the *set2* mutant germ cells would no longer carry *ovo*^{D} and thus should produce oocytes that would lack any maternal *Set2* mRNA or protein. Despite recombination to remove *ovo*^{D} from germ cells, no functional oocytes were produced, demonstrating that *Set2* is essential for oogenesis (data not shown). Therefore, the maternal contribution of *Set2* remains in our studies; its elimination might reveal an even more significant role or H3K36me3 in MSL recruitment than we have reported.

Recombinant MSL3 Binds Preferentially to Nucleosomes Trimethylated at H3K36

Eaf3, the yeast member of the conserved MSL3/MRG family of proteins, has been implicated in a physical and functional interaction of Rpd3(S) complexes with H3K36me3, raising the attractive hypothesis that MSL3 plays an analogous function in MSL complex. Furthermore, one distinction between high-affinity MSL binding sites such as *roX1*, *roX2*, and *18D11* and the majority of MSL targets is that high-affinity sites are MSL3 independent. Therefore, sensitivity to loss of H3K36me3 might be a specific characteristic of MSL3-dependent targets. To test the idea that MSL3 contributes to specific recognition of H3K36me3-modified nucleosomes, we performed gel shift analyses with recombinant MSL3 protein produced in baculovirus using nucleosomes assembled in vitro (Figure 6). Using an EMSA assay system where specifically modified recombinant nucleosomes were assembled (Li et al., 2007a), we found that purified MSL3 protein showed increased affinity to nucleosomes pretreated with active Set2, and thus marked with H3K36 methylation, as opposed to nucleosomes that were unmodified at H3K36. This preferential

binding was only detected in nucleosomes bearing linker DNA, suggesting that affinity for free DNA may be contributing to the binding of MSL3 to the nucleosomes methylated at H3K36. Titrations were performed to measure the relative affinity of MSL3 association with methylated compared to unmethylated nucleosomes. The increased affinity of MSL3 for methylated nucleosomes is best observed at the 4.4 nM concentration (Figure 6, lanes 2 and 6). These results provide additional evidence supporting a model in which H3K36me3 is a 3′ chromatin mark required for the robust, wild-type MSL binding pattern on the X chromosome.

DISCUSSION

Ectopic spreading of MSL complex to the 3′ ends of transcribed genes on autosomes indicates that a sequence-independent mechanism can define MSL complex target genes. Furthermore, trimethylation of H3K36 is required for optimal MSL complex targeting to transcribed genes on the male X chromosome subsequent to initial recognition of the X. In the absence of H3K36me3, MSL complex can associate with high-affinity sites on the X chromosome but exhibits reduced binding to target genes. Since MSL binding is reduced but is not eliminated, we favor a model in which association with H3K36me3 is a contributing factor that functions with recognition of one or more additional 3′ features of transcribed genes such as nascent mRNAs or RNA Pol II CTD phosphorylation.

In addition to a function for *Set2* in MSL complex targeting, our study demonstrates that *Set2* is essential for viability of both sexes in *Drosophila*. Conservation of the *Set2* H3K36 methyltransferase function from *S. cerevisiae* to *Drosophila* was observed, as predicted by sequence conservation (Morris et al., 2005). A variety of roles have been reported for Set2 in several organisms. In *Neurospora*, *S. pombe*, and NIH 3T3 cells, Set2 is required for optimal growth rate (Morris et al., 2005; Adhvaryu et al., 2005; Brown et al., 2006). The *S. cerevisiae set2Δ* mutant suppresses the loss of positive elongation factors (Biswas et al., 2006; Chu et al., 2006; Keogh et al., 2005). In *Drosophila*, mutants lacking zygotic *Set2* function fail to proceed through the developmental transitions from late larval to adult stages. The cause(s) of inviability in *Drosophila set2* mutants remains to be determined, but eyes composed entirely of homozygous *set2* mutant tissue were small and rough, indicating defects in cell proliferation.

Our in vitro studies using recombinant MSL3 produced in baculovirus revealed preferential interaction with nucleosomes that were trimethylated at H3K36, suggesting that a direct interaction may occur between MSL complex and H3K36me3 chromatin on the X chromosome. In *S. cerevisiae*, an MSL3 homolog, Eaf3, mediates an interaction between the Rpd3(S) complex and H3K36me3 at active genes (Carrozza et al., 2005; Keogh et al., 2005). If conserved, this function in *Drosophila* presumably would be played by another MSL3 family member, MRG15. In *S. cerevisiae*, Rpd3(S) is thought to deacetylate histones in the wake of RNA polymerase II to prevent uncontrolled activation and transcription initiation from cryptic start sites within genes (Carrozza et al., 2005). This raises the possibility that, on the X chromosome, MSL complex might compete for binding to H3K36me3 with the repressive deacetylation function of Rpd3(S). Alternatively, H3K36me3 may simply be a mark utilized by MSL complex to regulate target genes by a mechanism independent of Rpd3(S).

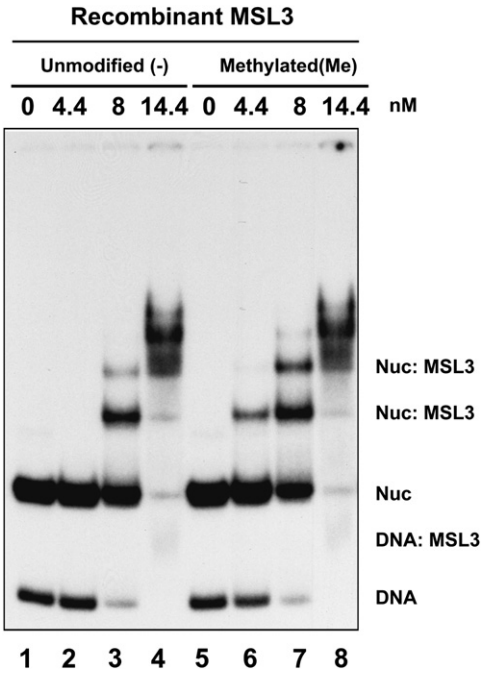

Figure 6. MSL3-TAP Interacts Specifically with H3K36me3 In Vitro

Xenopus histones were assembled into nucleosomes on a 216 bp DNA template by salt dilution, methylated with yeast Set2 protein, and used in a gel shift with baculovirus MSL3-TAP protein (Experimental Procedures). Titrations were performed to determine the specificity of the interaction between MSL3-TAP and methylated nucleosomes. MSL3-TAP exhibits a higher affinity for nucleosomes that have been methylated on H3K36 by *S. cerevisiae* Set2 (compare lanes 2 and 6). The concentration of MSL3-TAP is listed on the top of the figure, and the species formed are listed on the right.

H3K36me3 marks transcribed genes independent of transcript level but is a weak modulator of endogenous transcript and RNA polymerase II levels (Figure 1D, Figure S6) (Krogan et al., 2003; Rao et al., 2005; Kim et al., 2007; Li et al., 2007b). In *S. cerevisiae*, where its role is best understood, Set2 functions to suppress formation of aberrant internal transcripts by facilitating histone deacetylation yet has only small effects on endogenous transcript levels (Carrozza et al., 2005; Li et al., 2007a). In *Drosophila*, we detected small but reproducible changes in transcript levels at MSL complex target genes in *set2* mutant larvae (Figure S6). Also, we detected minimal changes in RNA Pol II levels as previously reported for the *set2Δ* mutant in *S. cerevisiae* (Figure S6) (Krogan et al., 2003). Also, changes in transcription level due to loss of dosage compensation are small, with a maximal 50%

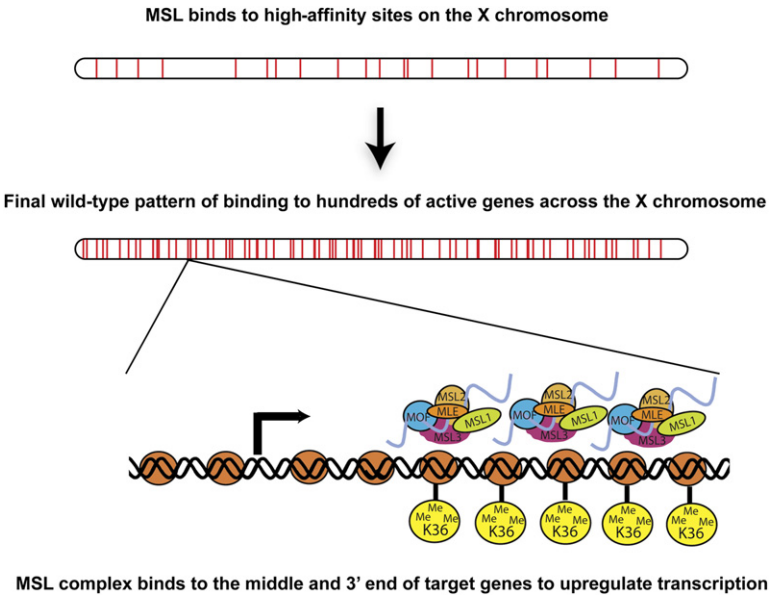

Figure 7. Model for Targeting of MSL Complex to Hundreds of Genes along the Male X Chromosome

In the early embryo, MSL complex associates with a set of 35–60 high-affinity sites, a process that is modulated by sequence elements and associated factors. Next, MSL complex identifies the majority of its targets: the middle and 3′ ends of hundreds of transcribed genes. Maximal association with target genes is modulated by the presence of the H3K36 trimethylation, which occurs by the action of the polymerase-associated Set2 histone methyltransferase. MSL complex then upregulates transcription of X-linked genes in males, thereby equalizing transcript levels between males and females.

decrease predicted (Hamada et al., 2005). Thus, the combined loss of the Set2 protein and reduction in MSL complex recruitment did not cause dramatic changes in transcript level (Figure S6). Furthermore, levels of H4Ac16 were decreased but not eliminated at target genes, consistent with residual MSL function that can explain why more dramatic changes in transcription of MSL complex target genes were not observed (Figure S6).

A defined mechanism for MSL complex targeting to hundreds of sites along the male X chromosome has remained elusive. Previous reports have posited two highly related models for MSL complex recruitment: a "spreading" model and an "affinities" model. Both models are based on the idea that specific MSL interaction occurs at high-affinity sites that mark the X chromosome. These sites have been mapped on polytene chromosomes, but most are not yet defined at the molecular level (Lyman et al., 1997; Kelley et al., 1999; Demakova et al., 2003; Oh et al., 2003; Dahlsveen et al., 2006). *roX* genes and other high-affinity sites are thought to concentrate MSL complex within an X chromosome domain. In the spreading model, MSL complex creates the full MSL binding pattern by searching the X chromosome for general characteristics of active genes without necessarily requiring a specific DNA sequence at each gene. This could occur either by scanning along the chromosome in a linear manner or by releasing and rebinding chromosomal regions in close physical proximity. We and others have previously demonstrated that *roX* RNAs can move in *trans* from one DNA molecule to another, so linear scanning is possible but not obligatory (Meller et al., 1997; Kelley et al., 1999; Fagegaltier and Baker, 2004; Oh et al., 2004; Dahlsveen et al., 2006;). The affinities model proposes that there is a continuum of affinity sites for MSL complex, ranging from high to low. Only when high-affinity sites are locally concentrated can low-affinity sites be recognized, similar to the spreading model (Demakova et al., 2003; Fagegaltier and Baker, 2004; Dahlsveen et al., 2006). The major difference is that even low-affinity sites are predicted to contain sequence elements that direct MSL binding. We believe our results documenting the pattern of ectopic MSL binding on chromosome 2L surrounding a *roX* transgene make the existence of sequence elements at every MSL binding site on the X chromosome unlikely. That the 2L pattern was analogous to that normally found on the X chromosome, targeting transcribed genes marked by H3K36me3 and binding with a 3′ bias, is strong evidence that MSL complex recognizes target genes marked by transcription. This does not exclude the possibility that transcribed genes carry common sequence elements but makes it unlikely that such sequence elements differ between autosomal genes and the majority of MSL target genes on the X chromosome.

In summary, our data are consistent with a model in which MSL complex first recognizes nascent *roX* transcripts and a series of high-affinity sequences along the male X chromosome and then scans the X for target genes that exhibit H3K36 trimethylation and other marks of active transcription (Figure 7). Recognition may involve the MSL3 chromodomain and additional factors. Trimethylation of H3K36 marks the middle and 3′ ends of transcription units, independent of absolute transcript levels in *Drosophila*, consistent with *S. cerevisiae* and mammalian systems (Rao et al., 2005; Kim et al., 2007). Thus, MSL complex recognition of H3K36me3 provides an important mechanism for identification of transcribed genes and avoidance of silenced regions.

EXPERIMENTAL PROCEDURES

Drosophila Stocks and Crosses

Flies were kindly provided by the Bloomington *Drosophila* Stock Center and were kept on a standard cornmeal-molasses medium at 25°C.

Details of mutant generation and genetic manipulations are described in the Supplemental Data.

ChIP-on-Chip and Standard ChIP from Tissue Culture Cells and Larvae

Chromatin was prepared from SL2 tissue culture cells and *Drosophila* larvae. The following antibodies were used for ChIP-on-chip or ChIP: (1) anti-H3 (ab1791); (2) anti-H3K36me3 (ab9050); (3) anti-H3K4me2 (ab7766) (Abcam); (4) anti-MSL2; (5) H4Ac16 (Serotec); and (6) anti-Pol II (non-phospho-specific (4H8) (Abcam). IgG beads were used for ChIP with the MSL3-TAP protein (Alekseyenko et al., 2006). ChIP and ChIP-on-chip protocols for cells and larvae are described in detail (Supplemental Data). A new computational approach was used to analyze ChIP-on-chip data and is described in the Supplemental Data (Peng et al., 2007). Data are available at the following website: http://www.chip.org/~ppark/Supplements/MC07.html.

Cell-Culture Methods and RNAi

Detailed protocols for cell culture and RNAi are provided in the Supplemental Data.

Western Blotting and Immunostaining of Polytene Chromosomes and Tissue Culture Cells

Detailed protocols are provided in the Supplemental Data.

mRNA Extraction and Quantitative Real-Time RT-PCR

Detailed protocols are provided in the Supplemental Data.

Nucleosome Gel Shift Analysis of MSL3 Interaction with H3K36me Nucleosomes

A detailed protocol is provided in the Supplemental Data.

Supplemental Data

Supplemental Data include Supplemental Experimental Procedures and six figures and can be found with this article online at http://www.molecule.org/cgi/content/full/28/1/121/DC1/.

ACKNOWLEDGMENTS

Many thanks to F. Winston, T. Sural, and C. Wang for important comments on the manuscript; O. Lee and J. Racine for excellent technical assistance; and M. Gelbart-Carey and S. Buratowski for helpful ideas and suggestions. We are grateful to H. Saumweber for antibodies. This work was supported by the National Institutes of Health (GM45744 to M.I.K and GM67825 to P.J.P), a grant to E.L. (a Leukemia and Lymphoma Society Fellow, 5198-05), and the Howard Hughes Medical Institute (HHMI). B.L. and J.L.W. are supported by a grant from the National Institutes of Health and funding from the Stowers Institute for Medical Research.

Received: May 12, 2007
Revised: June 5, 2007
Accepted: August 3, 2007
Published: October 11, 2007

REFERENCES

Adhvaryu, K.K., Morris, S.A., Strahl, B.D., and Selker, E.U. (2005). Methylation of histone H3 lysine 36 is required for normal development in *Neurospora crassa*. Eukaryot. Cell *4*, 1455–1464.

Alekseyenko, A.A., Larschan, E., Lai, W.R., Park, P.J., and Kuroda, M.I. (2006). High-resolution ChIP-chip analysis reveals that the *Drosophila* MSL complex selectively identifies active genes on the male X chromosome. Genes Dev. *20*, 848–857.

Bannister, A.J., Schneider, R., Myers, F.A., Thorne, A.W., Crane-Robinson, C., and Kouzarides, T. (2005). Spatial distribution of di- and tri-methyl lysine 36 of histone H3 at active genes. J. Biol. Chem. *280*, 17732–17736.

Barski, A., Cuddapah, S., Cui, K., Roh, T.Y., Schones, D.E., Wang, Z., Wei, G., Chepelev, I., and Zhao, K. (2007). High-resolution profiling of histone methylations in the human genome. Cell *129*, 823–837.

Bernstein, B.E., Meissner, A., and Lander, E.S. (2007). The mammalian epigenome. Cell *128*, 669–681.

Biswas, D., Dutta-Biswas, R., Mitra, D., Shibata, Y., Strahl, B.D., Formosa, T., and Stillman, D.J. (2006). Opposing roles for Set2 and yFACT in regulating TBP binding at promoters. EMBO J. *25*, 4479–4489.

Brown, M.A., Sims, R.J., 3rd, Gottlieb, P.D., and Tucker, P.W. (2006). Identification and characterization of Smyd2: a split SET/MYND domain-containing histone H3 lysine 36-specific methyltransferase that interacts with the Sin3 histone deacetylase complex. Mol. Cancer *5*, 26.

Carrozza, M.J., Li, B., Florens, L., Suganuma, T., Swanson, S.K., Lee, K.K., Shia, W.J., Anderson, S., Yates, J., Washburn, M.P., and Workman, J.L. (2005). Histone H3 methylation by Set2 directs deacetylation of coding regions by Rpd3S to suppress spurious intragenic transcription. Cell *123*, 581–592.

Chou, T.B., and Perrimon, N. (1992). Use of a yeast site-specific recombinase to produce female germline chimeras in *Drosophila*. Genetics *131*, 643–653.

Chu, Y., Sutton, A., Sternglanz, R., and Prelich, G. (2006). The BUR1 cyclin-dependent protein kinase is required for the normal pattern of histone methylation by SET2. Mol. Cell. Biol. *26*, 3029–3038.

Dahlsveen, I.K., Gilfillan, G.D., Shelest, V.I., Lamm, R., and Becker, P.B. (2006). Targeting determinants of dosage compensation in *Drosophila*. PLoS Genet. *2*, e5. Published online February 3, 2006. 10.1371/journal.pgen.0020005.

Daniel, J.A., Pray-Grant, M.G., and Grant, P.A. (2005). Effector proteins for methylated histones: an expanding family. Cell Cycle *4*, 919–926.

Demakova, O.V., Kotlikova, I.V., Gordadze, P.R., Alekseyenko, A.A., Kuroda, M.I., and Zhimulev, I.F. (2003). The MSL complex levels are critical for its correct targeting to the chromosomes in *Drosophila melanogaster*. Chromosoma *112*, 103–115.

Fagegaltier, D., and Baker, B.S. (2004). X chromosome sites autonomously recruit the dosage compensation complex in *Drosophila* males. PLoS Biol. *2*, e341. Published online October 5, 2004. 10.1371/journal.pbio.0020341.

Gilfillan, G.D., Straub, T., de Wit, E., Greil, F., Lamm, R., van Steensel, B., and Becker, P.B. (2006). Chromosome-wide gene-specific targeting of the *Drosophila* dosage compensation complex. Genes Dev. *20*, 858–870.

Hamada, F.N., Park, P.J., Gordadze, P.R., and Kuroda, M.I. (2005). Global regulation of X chromosomal genes by the MSL complex in *Drosophila melanogaster*. Genes Dev. *19*, 2289–2294.

Jenuwein, T., and Allis, C.D. (2001). Translating the histone code. Science *293*, 1074–1080.

Joshi, A.A., and Struhl, K. (2005). Eaf3 chromodomain interaction with methylated H3–K36 links histone deacetylation to Pol II elongation. Mol. Cell *20*, 971–978.

Kelley, R.L., Meller, V.H., Gordadze, P.R., Roman, G., Davis, R.L., and Kuroda, M.I. (1999). Epigenetic spreading of the *Drosophila* dosage compensation complex from roX RNA genes into flanking chromatin. Cell *98*, 513–522.

Keogh, M.C., Kurdistani, S.K., Morris, S.A., Ahn, S.H., Podolny, V., Collins, S.R., Schuldiner, M., Chin, K., Punna, T., Thompson, N.J., et al. (2005). Cotranscriptional set2 methylation of histone H3 lysine 36 recruits a repressive Rpd3 complex. Cell *123*, 593–605.

Kim, A., Kiefer, C.M., and Dean, A. (2007). Distinctive signatures of histone methylation in transcribed coding and noncoding human beta-globin sequences. Mol. Cell. Biol. *27*, 1271–1279.

Krogan, N.J., Kim, M., Tong, A., Golshani, A., Cagney, G., Canadien, V., Richards, D.P., Beattie, B.K., Emili, A., Boone, C., et al. (2003). Methylation of histone H3 by Set2 in *Saccharomyces cerevisiae* is linked to transcriptional elongation by RNA polymerase II. Mol. Cell. Biol. *23*, 4207–4218.

Legube, G., McWeeney, S.K., Lercher, M.J., and Akhtar, A. (2006). X-chromosome-wide profiling of MSL-1 distribution and dosage compensation in *Drosophila*. Genes Dev. *20*, 871–883.

Li, B., Gogol, M., Carey, M., Lee, D., Seidel, C., and Workman, J.L. (2007a). Combinatorial action of the Rco1 PHD domain and the Eaf3 chromodomain targets the Rpd3S complex to deacetylate transcribed chromatin. Science *316*, 1050–1054.

Li, B., Gogol, M., Carey, M., Pattenden, S.G., Seidel, C., and Workman, J.L. (2007b). Infrequently transcribed long genes depend on the Set2/Rpd3S pathway for accurate transcription. Genes Dev. *21*, 1422–1430.

Liu, C.L., Kaplan, T., Kim, M., Buratowski, S., Schreiber, S.L., Friedman, N., and Rando, O.J. (2005). Single-nucleosome mapping of histone modifications in *S. cerevisiae*. PLoS Biol. *3*, e328. Published online August 30, 2005. 10.1371/journal.pbio.0030328.

Lyman, L.M., Copps, K., Rastelli, L., Kelley, R.L., and Kuroda, M.I. (1997). *Drosophila* male-specific lethal-2 protein: structure/function analysis and dependence on MSL-1 for chromosome association. Genetics *147*, 1743–1753.

Meller, V.H., Wu, K.H., Roman, G., Kuroda, M.I., and Davis, R.L. (1997). *roX1* RNA paints the X chromosome of male *Drosophila* and is regulated by the dosage compensation system. Cell *88*, 445–457.

Morris, S.A., Shibata, Y., Noma, K., Tsukamoto, Y., Warren, E., Temple, B., Grewal, S.I., and Strahl, B.D. (2005). Histone H3 K36 methylation is associated with transcription elongation in *Schizosaccharomyces pombe*. Eukaryot. Cell *4*, 1446–1454.

Ng, K., Pullirsch, D., Leeb, M., and Wutz, A. (2007). Xist and the order of silencing. EMBO Rep. *8*, 34–39.

Oh, H., Park, Y., and Kuroda, M.I. (2003). Local spreading of MSL complexes from *roX* genes on the Drosophila X chromosome. Genes Dev. *17*, 1334–1339.

Oh, H., Bone, J.R., and Kuroda, M.I. (2004). Multiple classes of MSL binding sites target dosage compensation to the X chromosome of *Drosophila*. Curr. Biol. *14*, 481–487.

Park, Y., Kelley, R.L., Oh, H., Kuroda, M.I., and Meller, V.H. (2002). Extent of chromatin spreading determined by *roX* RNA recruitment of MSL proteins. Science *298*, 1620–1623.

Peng, S., Alekseyenko, A., Larschan, E., Kuroda, M., and Park, P.J. (2007). Experimental Design and Normalization for ChIP-chip Data. BMC Bioinformatics *8*, 219.

Pokholok, D.K., Harbison, C.T., Levine, S., Cole, M., Hannett, N.M., Lee, T.I., Bell, G.W., Walker, K., Rolfe, P.A., Herbolsheimer, E., et al. (2005). Genome-wide map of nucleosome acetylation and methylation in yeast. Cell *122*, 517–527.

Rando, O.J. (2007). Global patterns of histone modifications. Curr. Opin. Genet. Dev. *17*, 94–99.

Rao, B., Shibata, Y., Strahl, B.D., and Lieb, J.D. (2005). Dimethylation of histone H3 at lysine 36 demarcates regulatory and nonregulatory chromatin genome-wide. Mol. Cell. Biol. *25*, 9447–9459.

Stowers, R.S., and Schwarz, T.L. (1999). A genetic method for generating *Drosophila* eyes composed exclusively of mitotic clones of a single genotype. Genetics *152*, 1631–1639.

Strahl, B.D., Grant, P.A., Briggs, S.D., Sun, Z.W., Bone, J.R., Caldwell, J.A., Mollah, S., Cook, R.G., Shabanowitz, J., Hunt, D.F., and Allis, C.D. (2002). Set2 is a nucleosomal histone H3-selective methyltransferase that mediates transcriptional repression. Mol. Cell. Biol. *22*, 1298–1306.

Straub, T., and Becker, P.B. (2007). Dosage compensation: the beginning and end of generalization. Nat. Rev. Genet. *8*, 47–57.

Vakoc, C.R., Sachdeva, M.M., Wang, H., and Blobel, G.A. (2006). Profile of histone lysine methylation across transcribed mammalian chromatin. Mol. Cell. Biol. *26*, 9185–9195.

Vojnic, E., Simon, B., Strahl, B.D., Sattler, M., and Cramer, P. (2006). Structure and carboxyl-terminal domain (CTD) binding of the Set2 SRI domain that couples histone H3 Lys36 methylation to transcription. J. Biol. Chem. *281*, 13–15.

Yang, P.K., and Kuroda, M.I. (2007). Noncoding RNAs and intranuclear positioning in monoallelic gene expression. Cell *128*, 777–786.

Accession Numbers

Data are deposited at the National Center for Biotechnology Information Gene Expression Omnibus under accession number GSE8557.